Ionic liquid [BMIM][Cl] immobilized on cellulose fibers from pineapple leaves for desulphurization of fuels

Angélica M. Giorgi Perez[1], Marisol Fernández Rojas[1, 2], Luz A. Carreño Díaz[1]*

[1]*School of Chemistry, Faculty of Science, Universidad Industrial de Santander, Street 9, 27 Main Campus, Bucaramanga, 680002, Colombia*
[2]*School of Science and Engineering, Universidad de los Llanos, Km 12 Vía Puerto López, Villavicencio, Colombia*

*Corresponding author: Tel: (+57) (7) 6344000; E-mail: lcarreno@uis.edu.co

DOI: 10.5185/amlett.2019.2277
www.vbripress.com/aml

Abstract

Industrial combustion of fuels containing sulfur is responsible for most of the greenhouse gases in the atmosphere. The high impact of fuels is mainly on the content of aromatic S-compounds. These compounds are hard to remove through conventional hydrodesulphurization (HDS) processes because of their refractory properties and high boiling points. In this research, we are reporting the preparation, characterization, and evaluation of a cheap, regenerable and reusable composite based on the ionic liquid 1-butyl-3-methylimidazolium chloride immobilized on a renewable matrix of natural cellulose fibers. Characterization of the composite included FTIR, TGA, SEM, and XDR. The extraction capacity of thiophene and benzothiophene of the synthesized material was evaluated in synthetic mixes in isooctane and monitored by GC-FID. We achieved removal percentages of up to 62% of total sulfur from a model oil with an initial concentration of 458 mg S/L.

Keywords: Ionic liquids, pineapple leaves fibers, desulphurization, aromatic S-compounds.

Introduction

Air contamination is one of the most important consequences of industrial development in the last decades. Combustion of fuels has generated the acid rain and greenhouse effect by conversion of sulfur compounds into SO and SO_2 [**1**]. Those compounds in the air cause environmental damages as well as respiratory diseases, cancer, among others [**2**]. Hydrotreating, the conventional technology used at industrial level require hydrogen, and catalysts under aggressive conditions of pressure and temperature to break carbon-sulfur bonds [**3**]. With the purpose of contributing with a complementary and greener technology for sulfur removal from fuels, we worked with ionic liquids (IL) having good removal capacities of saturated and aromatic S-compounds depending on the used IL.

Nowadays, the focus of IL extraction processes for fuels is on aromatic sulfur compounds, which are difficult to remove, by common HDS. This kind of direct extractive desulfurization based on IL has higher percentages of removal than conventional organic solvents but still low desulfurization efficiency (10-40%) in a single extraction, so it requires several continuous extraction steps to reach the ideal S-concentrations. Study of oxidative methods based on IL technology started with systems using IL as extractant [**4**–**8**], with acetic acid as a catalyst and H_2O_2 as oxidant. This kind of systems allow removal of up to 99%, but the use of acetic acid make difficult the separation or regeneration of the catalyst, and there is oil contamination by dissolution of the catalyst at trace levels. A better alternative is the use of Lewis and Bronsted acidic ILs, which have a double function as extractant and catalyst allowing removal percentages as high as 100% with recycling of the IL up to six times; however, there is no report about the properties of the fuel oils after the oxidative extracting process.

Recently, the ILs are being supported on solid materials like silica, polymers, graphite and activated carbon (AC) to obtain materials easily removed from the system and regenerable [**9**–**14**]. Oxidative desulfurization in the solid state was reported with graphene-hexagonal boron nitride (G-h-BN) used as a support of tungsten ionic liquid. The synthesized material showed to be thermos- and chemically stable; reaction conditions were very mild, and sulfur removal of DBT from model oil could reach up to 98.5% at 60 °C. The catalyst could be recycled five times without significant loss of catalytic efficiency demonstrating a new strategy of designing high activity heterogeneous catalyst for organic reactions [**12**].

We studied liquid-liquid extractions of sulfur compounds achieving removal percentages of up to 61.2% y 69.8% for thiophene and dibenzothiophene using the pure ionic liquid [BMIM][BF_4]. To improve this percentage of removal and to obtain a cheap solid material, regenerable and reusable, then we prepared a composite supporting this IL on oxidized activated carbon. With this material, the extraction of thiophene and benzothiophene model oil at the optimal conditions was up to 80% using significantly less amount of IL [**15**]**.** In this research, we report a new composite material based on the IL [BMIM][Cl] immobilized on natural cellulose fibers for the extraction of sulfur compounds. To our knowledge, this is the first cellulose biocomposites based on an IL immobilized on cellulose. We characterized the composite material by TGA-DSC, SEM, FTIR, and XRD and evaluated it to determine the extraction capacity. The material extracted up to 72% (mainly thiophene) from an isooctane solution with an initial concentration of 458 mg S/L.

Experimental

Materials

Pineapple (Ananas comosus MD2) leaves collected from a market in Bucaramanga, Colombia. Sodium hydroxide, NaOH, (León Laboratories Ltda) 1-butyl-3-methylimidazolium chloride ([BMIM][Cl], for synthesis, Merck). Maleic Anhydride (Alpha Aesar), Isooctane (Merck), Thiophene (Merck), THF (Merck), DMF (Merck), HCl (Merck), Acetone (Merck). GC gases (nitrogen, hydrogen, helium, and air (99.999%) from Cryogas.

Pineapple leaves extraction, cleaning, and chemical alkaline treatment

Fibers were manually obtained from pineapple leaves, washed in an ultrasound bath for 1 hour at room temperature and dried (60 °C, 24 hours). Alkaline treatment on natural fibers disrupts hydrogen bonding in the network structure, increasing surface roughness; it is able of removing lignin, wax, and oils covering the external surface, depolymerizes cellulose and exposes the short length crystallites [**16**]. Also, aqueous sodium hydroxide (NaOH) is capable of promoting the ionization of the hydroxyl group to the corresponding alkoxide [**17, 18**]. For alkaline treatment, we immersed the raw fibers (RF) in 5% NaOH solution for 3h, then washed and dried to obtain the alkaline fibers (AF).

Treatment of Alkaline Cellulose Fibers with Maleic Anhydride and Immobilization of [BMIM][Cl] on treated fibers

Glucose is an aldohexose with a $–CH_2$ OH group in position C6; with the purpose of generating more active sites for the IL immobilization, the surface of the fiber was chemically modified. We mixed 2g of alkaline fibers were mixed in a solution of 2g of maleic anhydride dissolved in 20 mL of acetone; the mix was under stirring for 1 hour at room temperature. Then, the fibers were filtered, washed, and dried for 2 hours at 120 °C to obtain maleated fibers (AMF) [**19**].

Acidic groups were calculated by acid/base titration using the Boehm method to determine the effectiveness of the maleation reaction [**20**]. 1 g of AMF fibers was set in a beaker with 50 mL of NaOH 0,1 M (standardized with a solution of potassium biphthalate) under stirring at 30 ºC for five days; after that, we performed the back titration with HCl and phenolphthalein.

We performed the functionalization of AMF fibers with the ionic liquid by setting 1 g of AMF, and 0.5 g of the IL dissolved in 15 mL of DMF. The mix was under reflux at constant stirring for 6 hours, 70 °C in inert nitrogen atmosphere [**21, 22**]. Then the fibers were dried at 55 °C for 24 hours to obtain AMF/IL fibers [**23**].

Evaluation of the chemical stability of the material, AMF-IL

An important feature for the material is the chemical stability against lixiviation with solvents of variable polarity. There were tested three solvents: water, tetrahydrofuran (THF) and isooctane; for each experiment, we dried 0.1 g of the AMF/IL material in an oven for 1 hour at 115 ºC and then flushed it with portions of 3 mL of the solvent. We dried the material after each lixiviation for 1 hour at 115 °C. A qualitative test with silver nitrate $AgNO_3$ detected the presence of chloride in the lixiviated. For quantification: the first method was weight loss before and after each lixiviation-drying process. The second one, by UV-Vis at 213 nm which is the λ_{max} absorption for this IL using a calibration curve.

Materials characterization

For structural characterization, we used Fourier Transform Infrared spectroscopy (FT-IR) using a Perkin-Elmer Spectrum 100 spectrometer in ATR mode. By thermogravimetric analysis we determined the behavior and thermal stability of the composites; measurements performed under nitrogen atmosphere employing a TGA system from 40 to 600 °C at a heating rate of 20 °C/min in SDT-Q600 (TA Instrument). Field emission-SEM (FESEM) allowed determining the biomaterials morphology by using an Inspect F50 equipment (FEI Instruments) on secondary electrons mode. The materials crystallinity was calculated according to the Segal method [**24**] by XRD using a dust diffractometer BRUKER D8 ADVANCE with DaVinci geometry.

Evaluation of the material AMF-IL for desulfurization of model oil solutions

An experimental setup as shown in Figure S1 was used to evaluate the composite for removal of S-compounds from the model oil (MO) composed of thiophene (T) (415 mg S/L) and benzothiophene (BT) (43 mg S/L) for a total of 458 mg S/L dissolved in isooctane. For the experiments, we put the composite (0.15, 0.23, 0.37 and

0.71 g (±0.01 g)) in a fix bed quartz reactor with an internal diameter of 4 mm. The reactor temperatures evaluated were 25, 45, 65 and 75 °C (±1 °C) (Lindberg Blue Tube Furnace, Thermo Scientific). We pumped 10 mL of MO with a peristaltic pump (Masterflex easy-load) at a feed flow of 0.2 mL/min (±0.01 mL/min),). To determine reusability capacity of the spent composite, we used thermal desorption at 100 °C (±0.2 °C) for 24 hours after three cycles of extraction as regeneration process. The regenerated material was re-tested under the same experimental conditions.

Results and discussion

Chemical and spectroscopic characterization

The natural fibers are composed of cellulose, lignin, hemicellulose, pectins, and chlorophyll, among others [**25**]. The number of acidic groups on the fibers surface increased from 56.40 mg NaOH/g for RF, to 86.79 and 103.19 mgNaOH/g for AF and AMF, respectively. As stated, alkaline treatment removes lignin and hemicellulose leaving the cellulose exposed and the anhydride maleic treatment anchors carboxylate groups to the cellulose surface on natural fibers.

We used Infrared Spectroscopy to monitor chemical changes on fibers after the chemical treatments and the IL support (**Fig. 1**). The infrared spectrum of raw fibers, showed typical cellulose, lignin, and hemicellulose signals [**25–27**]. As expected after alkaline treatment, spectra showed the disappearance of the signals at 1730 cm^{-1} from C=O stretching of hemicellulose, at 1242 cm^{-1} from the C-O bond in lignin, and the typical bands of components such as lignin and pectins between 1650-1450 cm^{-1} [**28**]. Bands at 1029 and 1157 cm^{-1} originating from C-O and C-O-C bonds stretching in cellulose appear more intense, confirming that after the treatment the cellulose is exposed. The alkaline treatment also reduced the intensity of the OH band at 3311 cm^{-1} by removal of hydroxyl groups present in hemicellulose and lignin [**26**]. We also monitored the maleic reaction treatment by FTIR-ATR (**Fig. 1**).

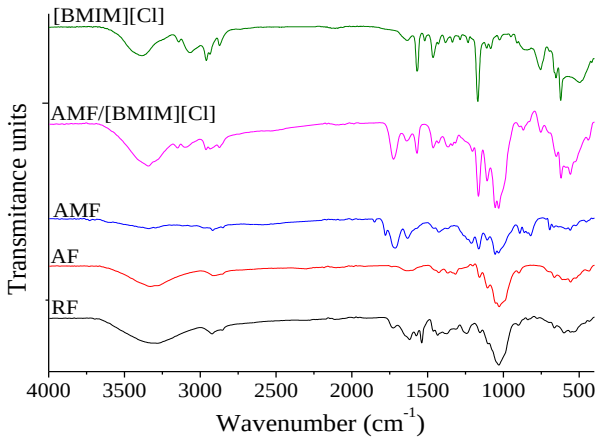

Fig. 1. FTIR spectra of raw fibers (RF), alkaline fibers (AF), maleate fibers (AMF), the pure IL [BMIM][Cl] and the composite material AMF/IL.

The spectrum of AMF shows how the broad O-H signal at 3345 cm^{-1} diminishes from the alcoholic groups that have been replaced by carboxylate groups after the maleation reaction; the small band above 3000 cm^{-1} are assigned to double bond from maleic anhydride. The carbonyl groups stretching vibrations appear at 1855 cm^{-1}. Bands at 1776 cm^{-1} and 1711 cm^{-1} are the "ceto" groups both symmetrical and anti-symmetrical vibrations, and the absorption at 1629 cm^{-1} corresponds to C=C [**29-32**]. **Fig. 1** also shows the spectra of the IL and the composite AMF/[BMIM][Cl] for comparison purposes. The peaks at wavenumbers 2973 cm^{-1} and 2870 cm^{-1} are the aliphatic asymmetric and symmetric (C–H) stretching vibration due to methyl groups. A broad peak in the range 3330–3450 cm^{-1} is due to quaternary amine salt formation with chlorine. Peaks from 3000 to 3200 cm^{-1} are due to H-C4 and H-C5 stretching vibrations in the imidazolium ring. However, there is a shift of one of these bands concerning the pure IL also reported by [**33**]. Wavenumbers at 1636 cm^{-1} and 1600 cm^{-1} are due to C=C and C=N stretching. The peak at wavenumber 840 cm^{-1} is due to C–N stretching vibration. In the composite material spectrum appears the corresponding bands to the matrix, but the signal corresponding to maleic anhydride carbonyl group disappeared and there is also a shift of carbonyl "ceto" groups indicating interaction of these groups from the fibers with the IL. The spectrum of composite shows the presence of the ionic liquid on the fibers and that interaction occurs through the formation of hydrogen bonds [**34**].

Evaluation of the chemical stability of the composite with the addition of different volumes of water, isooctane, and THF (aprotic polar) showed that the material is non-stable in water with a mass loss of 19.15% after four extraction processes (**Fig. 2**). Confirming the H-bonding formation the material is stable against THF and isooctane which indicates that it will work fine for fuels desulfurization.

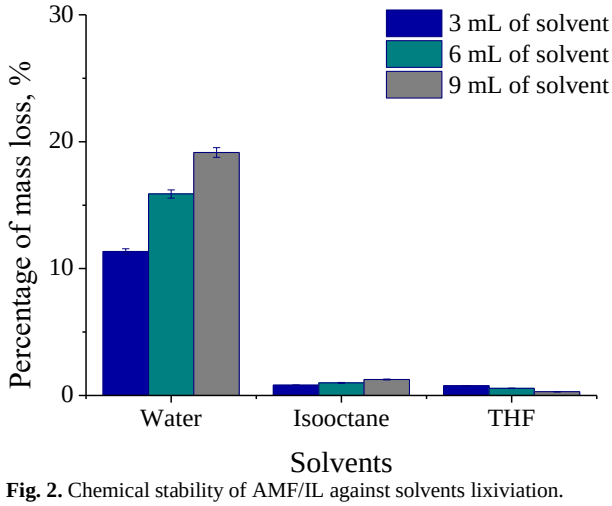

Fig. 2. Chemical stability of AMF/IL against solvents lixiviation.

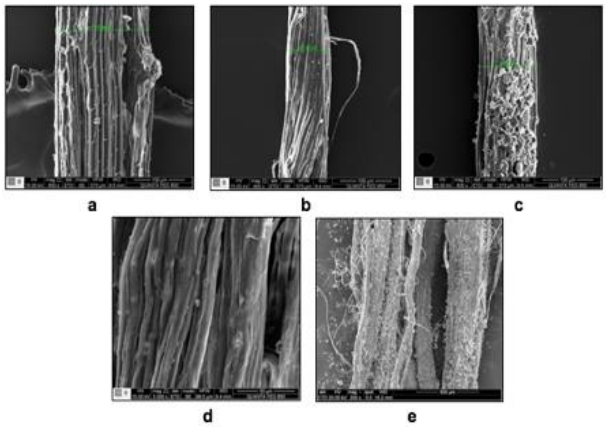

Fig. 3. SEM of cellulose fibers. A) RF; b) AF c) AMF d) AMF/IL e) AMF/IL after desulfurization.

Morphological characterization and crystallinity index

We monitored the changes in the fibers morphology by FESEM; **Fig. 3** shows the micrographs of fibers before and after chemical treatments, as well as, with IL and after the desulfurization process. **Fig. 3a** shows raw fibers image with a solid structure joined by lignin and hemicellulose components since these substances provide a firmer structure to the fiber [**17**]. For fibers with surface treatments, the SEM images showed a micro fibrillated structure which is related to the removal of lignin and hemicellulose, leaving free cellulose microfibrils and decreasing their thickness [**16, 34**], for raw fibers, the average diameter is 186.5 µm, while for alkaline fibers is 87.42 µm [**36**].

After the anhydride maleic treatment, the morphology of the surface of the fibers changed drastically as the average diameter was around 115.8 µm with small solid particles observed on the surface (see **Fig. 3c**). **Fig. 3d** shows a smoother surface of the final composite, which is related to the coating of the fibers with IL. A layer is covering the surface of the fiber and therefore decreasing the porosity of the material. **Fig. 3e** shows the fibers after the desulfurization process, the spectrum shows small particles adhered to the surface of the fiber [**36, 37**].

The diffraction patterns of RF, AF and AMF/IL are shown in **Fig. 4**, in which one are observable signals corresponding to crystalline and amorphous regions of the cellulose. From these diffraction patterns were calculated the crystallinity index with base in Segal method [**24**]. The crystallinity indexes of fibers increase with all the chemical treatments performed and were 0.80, 0.92 and 0.95 for RF, AF, and AMF/IL, respectively. These results indicate that regions of crystalline cellulose are greater than the amorphous ones. Additionally, different crystalline zones given by other peaks in the diffractogram are identified, for example for 2θ values between (14.5° - 15.3°) and (15.7° - 16.3°) [**38**]. Materials prepared with alkaline fibers showed higher crystallinity indexes than RF, indicating removal of lignin and hemicellulose. For the composite material, the IL seems to promote rearrangement of the amorphous fibers, increasing the crystallinity index [**38**].

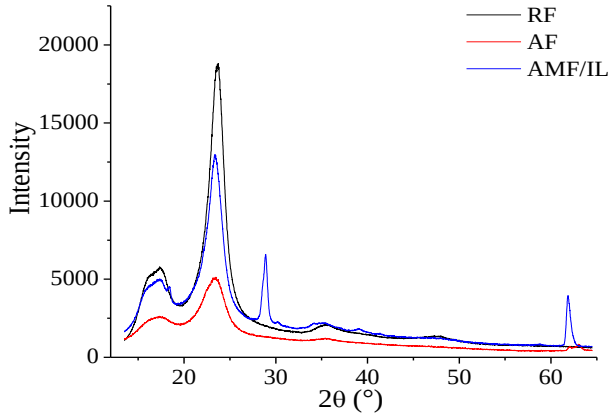

Fig. 4. XRD patterns of RF, AF and AMF/ILs.

Thermal characterization

Fig. 5 shows the thermograms of raw fibers, where the different stages of degradation occur between 0º to 800 ºC. During the first stage, there was a mass loss of 5, 7% between 0 and 123 ºC, attributed to dehydration of the fibers [**39**]. A mass loss of 68.31 % occurred during the second stage from 123 ºC to 381 ºC; assigned to degradation of holocellulose, hemicellulose, and lignin still present in the fibers. The third stage with a lost mass of 7,04% from 381 ºC to 782 ºC, corresponds to the degradation of cellulose due to depolymerization for glycosidic bonds breaking the chains of the natural polymer [**40**].

Fig. 5 also shows the thermograms of the fibers after the alkaline treatment, the maleic reaction treatment and after immobilization of the ionic liquid. As observed, these fibers showed similar thermal behavior. In addition to dehydration, three degradation steps occurred for all of them. After dehydration the next stage showed the highest mass loss, corresponding to depolymerization of the glycosidic bonds of the components such as cellulose, and lignin as well as, residual waxes, sugars, starches, pepsins and chlorophylls that were not removed by the manual extraction of the fibers. The next stage around 340 °C corresponds to the degradation of hemicellulose. Subsequently, the last stage starting at 390 °C corresponds to the degradation of cellulose and lignin, whose degradation occurs over a broader temperature range (250-900 °C) [**17, 38**].

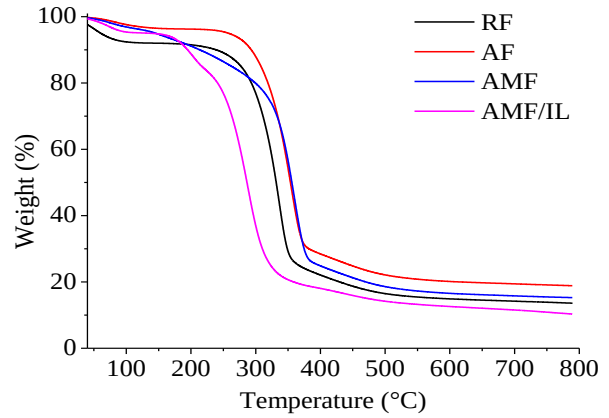

Fig. 5. TGA curves of RF, AF, AMF and AMF/IL.

As observed in **Fig. 5**, degradation of the material containing the ionic liquid occurs at a lower temperature, due to the thermal sensibility of the IL [BMIM][Cl]; In this material, the stage between 205 ºC – 394 ºC, with a higher mass loss of 69, 14%, is due to the breaking of intra and intermolecular bonds of the IL. The last stage for this material exhibited a low mass loss of 5.39%, from 394 ºC to 578 ºC as a result of the decomposition of the [BMIM][Cl] and the calcination of the remnant vegetable material [**41, 42**].

Desulfurization of model samples containing thiophene and benzothiophene

Variables studied included composite amount and temperature of extraction. From our expertise, the lower the flow, the higher the contact time, so we worked with the lower flow allowed by the pump, 0.2 mL/min.

Evaluation of the amount of composite and number of extraction cycles

The model oil sample consisted of a mix of 415.13 mg S/L (from thiophene) and 43.30 mg S/L (from benzothiophene) for a total S concentration of 458.43 mg/L. The amount of composite material changes the removal percentage as seen in **Fig. 6**. By increasing the number of cycles, the removal percentage increased until cycle 3, above that cycle the material was saturated.

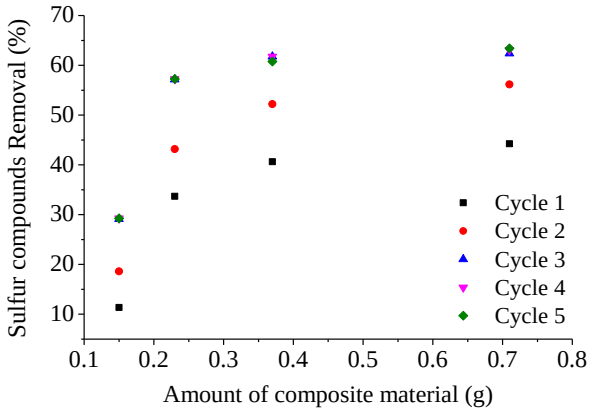

Fig. 6. Desulfurization of the model sample by changing the amount of composite material. *Experimental conditions: flow 0.2 mL/min, ambient temperature, initial concentration 458 mg S/L, three cycles of desulfurization.

The removal percentage of S-compounds is directly proportional to the amount of material used, however, by going from 0,37g to 0,71g of material in 3 cycles, it did not generate a significant increase in the removal percentage that was the reason to use 0.37 g of the composite for the next experiments using three cycles of extraction. The cost of the process changes by using just 1 or more cycles of extraction; in this experiment, we evaluated the effectiveness of using 1 cycle with more material against 3 cycles with a lower amount of material. This test showed that using 0.37 g of the material in 3 cycles of extraction allowed to obtain a removal percentage of 60.18% equivalent to use 1.123 g of the material in just one cycle of extraction (60.77%). By increasing the amount of composite 2.07 g with just one cycle of extraction, increased the removal percentage up to 72.25%, which was the higher removal obtained in this investigation.

Evaluation of temperature

We performed tests at four different temperature 25, 45, 65 and 75 °C, results showed in **Fig. S2** indicated that by increasing the temperature from ambient to 75 °C, the removal percentages decreased. The higher kinetic energy of the molecules diminished the interaction between the S-compounds and the active sites of the material. Experimenting at ambient temperature diminishes the process costs [**43**].

Discrimination of removal percentage by type of aromatic compound

The previous assays studied a mix of aromatic compounds (thiophene and benzothiophene) but the removal percentage was always expressed as total mg S/L. Several researchers stated that the extraction of aromatic compounds with imidazolium-based ionic liquids occurs by H-bonding (between the cation of the IL and the S atom of the sulfur compound) as proposed by Nie *et al.*[**44**] However, a good number of researchers concluded that the interaction between the IL and the S-compounds are π-π type between the π-electrons of imidazolium cation and the π-electrons of the S-compounds [**45-48**]. Using the experimental conditions established in the previous assays we determined the final concentration of each aromatic compound after each cycle of extraction by GC-FID and calibration curves for each compound.

Anantharaj and Banerjee *et al.* [**49-51**] stated that the volume and shape of the IL determined the type of interactions between the cation of the IL and the aromatic ring of the S-compound based on steric hindrance. In this research, we found that by supporting the IL on the cellulose fibers, there is selectivity toward thiophene (as shown in **Table 1**). Using pure IL for S-compounds extraction, it showed selectivity of the active sites toward compounds with the greater number of π electrons (in this case benzothiophene) however, in this case, it seems that the steric hindrance favored interaction between the IL and the smaller S-compound as stated by Su *et al.* [**52, 53**].

Table 1. Desulfurization of a model sample containing thiophene and benzothiophene[a].

Sample	Cycle #	Concentration (mg S/L)	Sulfur Removal (%)
Thiophene[b]	1	228,68	44,91
	2	176,27	57,54
	3	132,84	58,00
Benzothiophene[c]	1	41,71	3,67
	2	41,47	4,23
	3	41,43	4,32

[a] Experimental Conditions: Temperature 25 °C; Flow 0,2 mL/min; Amount of composite 0,37 g; Total cycles 3. [b] initial concentration: 415,31 mgS/L from Thiophene, [c] initial concentration: 43,30 mg S/L from Benzothiophene

Study of regeneration and reuse of the composite material

Industrialization of this extraction process requires regeneration and reuse of the materials. To study if the composite material could be regenerated once it gets saturated and reuse it, this one was subjected to five extraction cycles, then was thermally regenerated and retested. **Table 2** shows that after cycle #3 the material got saturated ant that after regeneration, the material lost 10% of removal capacity indicating that can be reused.

Table 2. Extraction of S-compounds with new and regenerated composite.

Cycles #	Sulfur removal (%)	
	New material	Regenerated material
1	40,63	37,26
2	52,19	40,75
3	61,74	50,09
4	61,76	49,67
5	60,75	49,45

Experimental Conditions: Temperature 25 °C; Flow 0,2 mL/min, V sample 10 mL, amount of material 0.37g.

Conclusions

The IL [BMIM] [Cl] was immobilized on chemically treated cellulose fibers, which was confirmed by means of DRX, FTIR, SEM, and TGA. The cellulose-IL composite was used for desulfurization of model solutions of 458 ppm of total S-contributed by thiophene and benzothiophene and removal percentages of up to 61.7% were obtained. The best desulfurization percentage was achieved at 25 ºC, with a flow of 0.2 mL/ min and 0.37g of synthesized material in 3 desulfurization cycles. It was determined that once saturated composites can be regenerated by thermal treatment with a loss of 10% efficiency.

Acknowledgments

Authors thank XRF and Microscopy Laboratories for all analysis performed, and the excellent service during data acquisition at Guatiguará Technology Park - UIS. Authors also thank Vice-rectorate for Research and Extension, Research Laboratory for Sustainable Chemistry and the Universidad Industrial de Santander.

Author's contributions

Conceived the plan: A.P., M.R., L.D.; Performed the experiments: A.P; Data analysis: A.P., M.R.; Wrote the paper: M..R., L.D. Authors have no competing for financial interests.

Supporting information

Supporting information are available from VBRI Press.

References

1. Ibrahim, M.; Hayyan, M.; Hashim, M.; Hayyan, A., *Renewable and Sustainable Energy Reviews* **2017**, *76*, 1534. **DOI:** 10.1016/j.rser.2016.11.194
2. Gavidia, T.; Pronczuk, J.; Sly, P., *Revista Chilena de enfermedades respiratorias* **2009**, *25*, 99. **DOI:** 10.4067/S0717-73482009000200006
3. Barbosa, A.; Vega, A., de Rio A. Avances en Ciencias e Ingeniería **2014**, 5, 37.
4. Zhang, W.; Xu, K.; Zhang, Q.; Liu, D.; Wu, S.; Verpoort, F., Song, X., *Ind. Eng. Chem. Res.* **2010**, *49*, 11760. **DOI:** 10.1021/ie100957k
5. Lu, L.; Cheng, S.; Gao, J.; Gao, G.; He, M., *Energy and Fuels* **2007**, *21*, 383. **DOI:** 10.1021/ef060345o
6. Yu, G.; Zhao, J.; Song, D.; Asumana, C.; Zhang, X.; Chen, X.; *Industrial & Engineering Chemistry Research* **2011**, *50*, 11690. **DOI:** 10.1021/ie200735p
7. Cun, Z.; Feng, W.; Xiao-yu, P.; Xiao-qin, L., *Journal of Fuel Chemistry and Technology* **2011**, *39*, 689. **DOI:** 10.1016/S1872-5813(11)60041-8
8. Gao, H.; Guo, C.; Xing, J.; Zhao, J.; Liu, H., *Green Chem* **2010**, *12*, 1220. **DOI:** 10.1039/c002108c
9. Jiang, W.; Zheng, D.; Xun, S.; Qin, Y.; Lu, Q.; Zhu, W.; Li, H., *Fuel* **2017**, *190*, 1. **DOI:** 10.1016/j.fuel.2016.11.024
10. Severa, G.; Bethune, K.; Rocheleau, R.; Higgins, S., *Chemical Engineering Journal* **2015**, *265*, 249. **DOI:** 10.1016/j.cej.2014.12.051
11. Carvalho, A.S.; Conto, J.F.; Campo,s K.; Oliveira, M., In X Encontro Brasileiro sobre Adsorcao, Guarujá, **2014**, 16.
12. Dai, B.; Wu, P.; Zhu, W.; Chao, Y.; Sun, J.; Xiong, J., *RSC Advances* **2016**, *11*, 140. **DOI:** 10.1039/c5ra23272d
13. Rojas, M.; Bernard, F.; Aquino, A.; Borges, J.; Vecchia, F.; Menezes, S.; Ligabue, R.; Einloft, S., *J of Mol. Cata. A: Chemical* **2014**, *392*, 83. **DOI:**10.1016/j.molcata.2014.05.007
14. Plata, J.F.; Carreno, L.A., *Materials Research* **2016**, *19*, 534. **DOI:** 10.1590/1980-5373-MR-2015-0561
15. Cogollo, M.; Salazar, M.; Cely, M.; Pinill, A.; Ardila, J.; Fernandez, M.; Carreno, L.A., *Advanced Materials Letters* **2018**, *9*, 488. **DOI:** 10.5185/amlett.2018.2065
16. Liu, X.; Chang, P.R.; Zheng, P.; Anderson, D.; Ma, X., *Cellulose* **2015**, *22*, 709. **DOI:** 10.1007/s10570-014-0467-0
17. Kabir, M.; Wang, H.; Lau, K.; Cardona, F., *Composites Part B: Engineering* **2012**, *43*, 2883. **DOI:** 10.1016/j.compositesb.2012.04.053
18. Li, X.; Tabil, L.; Panigrahi, S., *Journal of Polymers and the Environment* **2007**, *15*, 25. **DOI:** 10.1007/s10924-006-0042-3
19. Bernard, F.; Rodrigues, D.; Polesso, B.; Donato, A.; Seferin, M.; Chaban, V.; Dalla Vecchia, F.; Einloft, S., *Fuel Processing Technology* **2016**, *149*, 131. **DOI:** 10.1016/j.fuproc.2016.04.014
20. Briceño, N.; Guzmán, M.; Díaz, J., *Revista Colombiana de Química* **2007**, *36*, 121. **DOI:** 10.15446/rev.colomb.quim
21. Swatloski, R.; Spear, S.; Holbrey, J.; Rogers, R., *J. Am. Chem. Soc*. **2002**, *124*, 4974. **DOI:** 10.1021/ja025790m
22. Hong, C.; Kim, N.; Kang, S., *Plastics Rubber and Composites* **2008**, *37*, 325. **DOI:**10.1179/174328908X314334
23. Alvarez, J.; Rey, R.; Acosta, R., *Revista ION* **2012**, *25*, 61.
24. Segal, L.; Creely, J.; Martin, A.; Conrad, C., *Textile Research Journal* **1959**, *29*, 786. **DOI:** 10.1177/004051755902901003
25. Abdel-Halim, E., *Arabian Journal of Chemistry* **2014**, *7*, 362. **DOI:** 10.1016/j.arabjc.2013.05.006
26. Fan, M.; Dai, D.; Huang, B., Fourier Transform Infrared Spectroscopy for Natural Fibres, In Fourier Trasnform; Salih, S. (Ed); InTech **:** Croatia **2012**, 45. **DOI:** 10.5772/35482
27. Kabir, M., Effects of Chemical Treatments on Hemp Fibre Reinforced Polyester Composites **2012**, 232.
28. Benhamou, K.; Kaddami, H.; Magnin, A.; Dufresne, A.; Ahmad, A., *Carbohydrate Polymers* **2015**, *122*, 202. **DOI:** 10.1016/j.carbpol.2014.12.081
29. Mohanty, A.; Misra, M.; Drzal, L.; Selke, S.; Harte, B.; Hinrichsen, G.; (Eds.)., Natural Fibers, Biopolymers, and

Biocomposites; CRC Press**:** USA, **2005**.
30. Faruk, O.; Bledzki, A.; Fink, H.; Sain, M., *Progress in Polymer Science* **2012**, *37*, 1552.
DOI:10.1016/j.progpolymsci.2012.04.003
31. Olivares, R.; Luis, J.; Vázquez Rodríguez, S.; Zabaleta, L.; Rosalba, A.; Sánchez Valdes, S., Ingenierías **2008**, *11*, 47.
32. Guzmán, M.; Murillo, E. A., *Polímeros* **2014**, 24, 162.
DOI: 10.4322/polimeros.2014.034
33. Dharaskar, S. A.; Wasewar, K. L.; Varma, M. N.; Shende, D. Z.; Yoo, C. K., *Arabian Journal of Chemistry* **2016**, *9*, 578.
DOI: 10.1016/j.arabjc.2013.09.034
34. Wang, P.; Liu, S.; Lu, L.; Ma, X.; He, Y.; Deng, Y., *RSC Adv*. **2015**, *5*, 62110.
DOI: 10.1039/C5RA09281G
35. Bernard, F.; Polesso, B.; Cobalchini, F.; Donato, A.; Seferin, M.; Ligabue, R.; Chaban, V., do Nascimento J.; Dalla Vecchia, F.; Einloft, S., *Polymer* **2016**, *102*, 199.
DOI: 10.1016/j.polymer.2016.08.095
36. Mina, J., Biotecnología en el Sector Agropecuario y Agroindustrial **2012**, *10*, 99.
37. Panyasart, K.; Chaiyut, N.; Amornsakchai, T.; Santawitee, O., *Energy Procedia* **2014**, *56*, 406.
DOI:10.1016/j.egypro.2014.07.173
38. Poletto, M.; Júnior, H.; Zattera, A., *Materials* **2014**, *7*, 6105.
DOI: 10.3390/ma7096105
39. Enríquez, C.; Velasco, M.; Ortiz, V., *Biotecnología en el Sector Agropecuario y Agroindustrial* **2012**, *10*, 182.
40. Canché-Escamilla, G.; De los Santos-Hernández, J.; Andrade-Canto, S.; Gómez-Cruz, R., *Información tecnológica* **2005**, *16*, 83.
DOI: 10.4067/S0718-07642005000100012
41. Yassin, F.; El Kady, F.; Ahmed, H.; Mohamed, L.; Shaban, S.; Elfadaly, A., *Egyptian Journal of Petroleum* **2015**, 24, 103.
DOI: 10.1016/j.ejpe.2015.02.011
42. Hao, Y.; Peng, J.; Hu, S.; Li, J.; Zhai, M., *Thermochimica Acta* **2010**, *501*, 78.
DOI: 10.1016/j.tca.2010.01.013
43. Shu, C.; Sun, T.; Zhang, H.; Jia, J.; Lou, Z., *Fuel* **2014**, *121*, 72.
DOI:10.1016/j.fuel.2013.12.037
44. Nie, Y.; Yuan, X., *Theor. Comput. Chem*. **2011**, *10*, 31.
DOI: 10.1142/S0219633611006268
45. Zhang, S.; Zhang, Q.; Zhang, Z., *Ind. Eng. Chem.* Res. **2004**, *43*, 614.
DOI: 10.1021/ie030561+
46. Mecozzi, S.; West, A.; Dougherty, D., *Proc. Natl. Acad. Sci. U.S.A.* **1996**, *93*, 10566.
DOI: 10.1073/pnas.93.20.10566
47. Nie, Y.; Li, C.; Wang, Z., *Ind. Eng. Chem. Res*. **2007**, *46*, 5108.
DOI: 10.1021/ie070385v
48. Holbrey, J.; López-Martin, I.; Rothenberg, G.; Seddon, K.; Silvero, G.; Zheng, X., *Green Chem.* **2008**, *10*, 87.
DOI: 10.1039/B710651C
49. Anantharaj, R.; Banerjee, T., *AIChE J.* **2011**, *57*, 749.
DOI: 10.1002/aic.12281
50. Zhao, H.; Baker, G.; Wagle, D.; Ravula, S.; Zhang, Q., *ACS Sustainable Chem. Eng.* **2016**, *4*, 4771.
DOI: 10.1021/acssuschemeng.6b00972
51. Hirota, M.; Sakaibara, K.; Suezawa, H.; Yuzuri, T.; Ankai, E.; Nishio, M., *J. Phys. Org. Chem.* **2000**, *13*, 620.
DOI: 10.1002/1099-1395(200010)13**:**10
52. Su, B.; Zhang, S.; Zhang, Z., *The Journal of Physical Chemistry B* **2004**, *108*, 19510.
DOI: 10.1021/jp049027l
53. Anantharaj, R.; Banerjee, T., *Fuel Processing Technology* **2011**, *92*, 39.
DOI:10.1016/j.fuproc.2010.08.018

